

Chapter 2

A Stefan problem with moving phase change material, variable thermal conductivity and periodic boundary condition

2.1 Introduction

A Stefan problem (moving boundary problem), describing the process of phase change, is one of the interesting problems from the mathematical and industrial point of view due to its nonlinear nature even in its simplest form and presence of moving phase boundary/front. The moving phase front is a part of the solution, so it has to be calculated from the energy balance condition described at the moving phase front which is often called as Stefan condition. Due to the involvement of Stefan condition in the problems, these problems are frequently known as Stefan problems. There are several practical processes that are governed by moving boundary problem, such as freezing of ice, melting of material, preservation of foods, recrystallization of metals, thermal energy storage, oxygen diffusion process, etc. The mathematical models of classical moving boundary problems, its solutions, and applications are well covered in [3, 99, 100].

Moving boundary problems with new thermo-physical properties of the phase change material have been attracted many investigators [76, 101, 102, 79, 103, 104] in last century that can be observed as the modification in the classical problems. Recently, Kumar et al. [87] presented a moving boundary problem with time and temperature dependent thermal conductivity. Ceretani et al. [84] discussed a phase change problem with temperature-dependent thermal conductivity and presented an exact solution to the problem. A phase change problem involving temperature-dependent specific heat and thermal conductivity is also presented by Kumar et al. [88]. In 2005, Jou et al. [105] discussed size-dependent thermal conductivity of a solid from the Extended Irreversible Thermodynamics theory [106]. Based on this fact, Font [46] and Calvo-Schwarzwalder [107] also analyzed a mathematical model of a moving boundary problem in which he assumed a variable thermal conductivity that is a function of moving interface, and discussed approximate solutions to the problem via perturbation and numerical approaches. Moving boundary problems with moving phase change material (PCM) arise in many phase change processes, but only a few investigators [108, 109] considered the phase change problem with moving PCM. Recently, Turkyilmazoglu [110] discussed the analytical solutions to the phase change problems with unidirectional moving phase change material by assuming constant thermo-physical properties of the material. After that Singh et al. [111] discussed a phase change problem with convective boundary condition, moving phase change material and variable thermal coefficients. Singh et al. [112] also discussed a melting problem with Dirichlet's boundary condition that includes moving phase change material and variable thermal coefficients.

In this study, based on previous observations, a moving boundary problem is considered with moving PCM and variable thermal conductivity that depends on moving

interface. Moreover, a periodic boundary condition is assumed at the first boundary, *i.e.* $x = 0$ which was earlier considered in the phase change problems by many researchers [113, 114, 66, 115, 116, 117]. The exact solution of a moving boundary problem with periodic boundary condition is not available even in its simplest form; therefore, a numerical solution based on finite difference method to our problem is presented to determine temperature profile in the domain and moving phase boundary during the phase change process. Numerical schemes to these problems require a special care, and sometime a very small mesh size and time step size are often required for the accuracy of the solutions [118, 119]. In the literature, many researchers used either finite element method or finite difference method or integral method to present numerical solution to the moving boundary problems with different kinds of boundary conditions, some of them are given in the references [120, 121, 51, 122, 123, 67, 124, 125].

2.2 Mathematical Model

Here, a melting problem of a solid is considered which is initially at its equilibrium melting temperature F_m . It is assumed that the edge at $z = 0$ is suddenly subjected to a time-dependent temperature $F_0(\tau)$ which is higher than F_m . As time proceeds, the solid starts to melt and a moving melting front (moving boundary) is formed which propagates along the positive z direction. Besides the classical melting problem, it is assumed that the phase change material moves with a speed of u [110]. The temperature distribution in molten region can be described by the following

mathematical model:

$$\rho c \left(\frac{\partial F}{\partial \tau} + u \frac{\partial F}{\partial z} \right) = \kappa(S(\tau)) \frac{\partial^2 F}{\partial z^2}, \quad 0 < z < S(\tau), \quad \tau > 0 \quad (2.1)$$

$$F(0, \tau) = F_0(\tau), \quad (2.2)$$

$$F(S(\tau), \tau) = F_m, \quad (2.3)$$

$$\rho L \frac{dS}{d\tau} = -\kappa(S(\tau)) \frac{\partial F(S(\tau), \tau)}{\partial z}, \quad (2.4)$$

$$S(0) = 0. \quad (2.5)$$

where F is temperature profile in molten region, z is space, τ is time, ρ is density, c is the specific heat, u is the unidirectional speed depending on time, L is latent heat and S is the moving melting front.

Here, the size-dependent thermal conductivity is considered as

$$\kappa(S(\tau)) = \frac{2\kappa_0 S^2(\tau)}{l^2} \left(\sqrt{1 + \frac{l^2}{S^2(\tau)}} - 1 \right). \quad (2.6)$$

The expression of size-dependent thermal conductivity is derived from the theory of Extended Irreversible Thermodynamics by assuming equal phonon mean-free paths and relaxation times. The physical relevance of size-dependent thermal conductivity can be seen in [46] and [107].

2.2.1 Dimensionless form

To make the model in dimensionless form, the following transformations

$$T = \frac{F - F_m}{\Delta F_{ref}}, \quad x = \frac{z}{l}, \quad t = \frac{k_0}{l^2 \rho c} \tau, \quad s = \frac{S}{l}, \quad u = Pe \sqrt{\frac{\kappa_0}{\rho c T}} \quad (2.7)$$

are substituted in the Eqs. (1)-(5), which give

$$\frac{\partial T}{\partial t} + \frac{Pe}{\sqrt{t}} \frac{\partial T}{\partial x} = 2s(\sqrt{s^2 + 1} - s) \frac{\partial^2 T}{\partial x^2}, \quad 0 < x < s(t), t > 0, \quad (2.8)$$

$$T(0, t) = \frac{F_0(\tau) - F_m}{\Delta F_{ref}} = f(t), \quad (2.9)$$

$$T(s(t), t) = 0, \quad (2.10)$$

$$\frac{1}{Ste} \frac{ds}{dt} = -2s(\sqrt{s^2 + 1} - s) \frac{\partial T(s(t), t)}{\partial x}, \quad (2.11)$$

$$s(0) = 0, \quad (2.12)$$

where $f(t) = 1 + \epsilon \sin(\omega t)$, $Ste = \frac{c\Delta F_{ref}}{L}$ is the Stefan number, $Pe = u\sqrt{\frac{\tau}{\alpha}}$ denotes the Peclet number and $\alpha = \frac{\kappa_0}{\rho c}$.

2.3 Numerical solution

First, the moving domain $[0, s(t)]$ is converted into the fixed domain $[0, 1]$ by using the following Landau-type transformation [99],

$$U(\zeta, t) = T(x, t), \quad \zeta = \frac{x}{s(t)}. \quad (2.13)$$

Under the transformation (2.13) our problem (2.8)-(2.12) reduce to the following system:

$$\frac{\partial U}{\partial t} - \frac{\zeta}{s(t)} \frac{ds}{dt} \frac{\partial U}{\partial \zeta} + \frac{Pe}{s(t)\sqrt{t}} \frac{\partial U}{\partial \zeta} = \frac{2(\sqrt{s^2 + 1} - s)}{s} \frac{\partial^2 U}{\partial \zeta^2}, \quad t > 0, \quad 0 < \zeta < 1, \quad (2.14)$$

$$U(0, t) = f(t) = 1 + \epsilon \sin(\omega t), \quad (2.15)$$

$$U(1, t) = 0, \quad (2.16)$$

$$\frac{1}{Ste} \frac{ds}{dt} = -2(\sqrt{s^2 + 1} - s) \frac{\partial U(1, t)}{\partial \zeta}, \quad (2.17)$$

$$s(0) = 0. \quad (2.18)$$

Now, the step size of time discretization is considered as $k = \Delta t$ and space discretization $h = \Delta \zeta = \frac{1}{P}$, where P is positive integer. The mesh points are taken as (ζ_i, t^n) , where $\zeta_i = ih$, $0 \leq i \leq P$ and $t^n = nk$, $n \geq 0$. The approximate value of $U(\zeta, t)$ at mesh point (ζ_i, t^n) is denoted as U_i^n and the approximate value of $s(t)$ at t^n is taken as s^n .

Let us approximate the time derivative and space derivative as

$$\frac{\partial U(\zeta_i, t^n)}{\partial t} \approx \frac{U_i^{n+1} - U_i^n}{k}, \quad \frac{ds(t^n)}{dt} \approx \frac{s^{n+1} - s^n}{k} \quad (2.19)$$

$$\frac{\partial U(\zeta_i, t^n)}{\partial \zeta} \approx \frac{U_{i+1}^n - U_{i-1}^n}{2h}, \quad \frac{\partial^2 U(\zeta_i, t^n)}{\partial \zeta^2} \approx \frac{U_{i+1}^n - 2U_i^n + U_{i-1}^n}{h^2}. \quad (2.20)$$

From Eqs.(2.19)-(2.20), the Eq.(2.14) is approximated by

$$\begin{aligned} & \frac{U_i^{n+1} - U_i^n}{k} - \frac{\zeta_i}{s^n} \left(\frac{s^{n+1} - s^n}{k} \right) \left(\frac{U_{i+1}^n - U_{i-1}^n}{2h} \right) + \frac{Pe}{s^n \sqrt{nk}} \left(\frac{U_{i+1}^n - U_{i-1}^n}{2h} \right) \\ & = \frac{2(\sqrt{s^{n2} + 1} - s^n)}{s^n} \frac{(U_{i+1}^n - 2U_i^n + U_{i-1}^n)}{h^2}, \quad n \geq 0, \quad 1 \leq i \leq P - 1, \end{aligned} \quad (2.21)$$

which can be arranged as

$$\begin{aligned} U_i^{n+1} &= \left[\frac{2k(\sqrt{s^{n2} + 1} - s^n)}{h^2 s^n} + \frac{Pe}{2hs^n} \sqrt{\frac{k}{n}} - \frac{k\zeta_i}{2hs^n} \left(\frac{s^{n+1} - s^n}{k} \right) \right] U_{i-1}^n \\ &+ \left[1 - \frac{4k(\sqrt{s^{n2} + 1} - s^n)}{h^2 s^n} \right] U_i^n + \left[\frac{2k(\sqrt{s^{n2} + 1} - s^n)}{h^2 s^n} - \frac{Pe}{2hs^n} \sqrt{\frac{k}{n}} \right. \\ &+ \left. \frac{k\zeta_i}{2hs^n} \left(\frac{s^{n+1} - s^n}{k} \right) \right] U_{i+1}^n, \quad n \geq 0, \quad 1 \leq i \leq P - 1. \end{aligned} \quad (2.22)$$

The Eqs. (2.15) and (2.16) become

$$U_0^n = 1 + \epsilon \sin(\omega nk), \quad \& \quad U_P^n = 0, \quad n \geq 0. \quad (2.23)$$

Using three point backward difference formula for space derivative and first order forward difference approximation for time derivative, the Stefan condition (2.17) becomes

$$\frac{s^{n+1} - s^n}{k} = -2Ste(\sqrt{s^{n2} + 1} - s^n) \frac{(U_{P-2}^n - 4U_{P-1}^n + 3U_P^n)}{2h}, \quad n \geq 0, \quad (2.24)$$

for the accuracy of order $\mathcal{O}(k) + \mathcal{O}(h^2)$.

From Eq.(2.23), the Eq.(2.24) can be rewritten as

$$s^{n+1} = s^n - 2kSte(\sqrt{s^{n2} + 1} - s^n) \frac{(U_{P-2}^n - 4U_{P-1}^n)}{2h}, \quad n \geq 0. \quad (2.25)$$

Now, using Eq.(2.25) in the Eq.(2.22), we have

$$U_i^{n+1} = a_i^n U_{i-1}^n + b_i^n U_i^n + c_i^n U_{i+1}^n, \quad n \geq 0, \quad 1 \leq i \leq P - 1, \quad (2.26)$$

where

$$a_i^n = \left[\frac{2k(\sqrt{s^{n2} + 1} - s^n)}{h^2 s^n} + \frac{Pe}{2hs^n} \sqrt{\frac{k}{n}} + \frac{k\zeta_i Ste(\sqrt{s^{n2} + 1} - s^n)}{s^n} \frac{(U_{P-2}^n - 4U_{P-1}^n)}{2h^2} \right], \quad (2.27)$$

$$b_i^n = \left[1 - \frac{4k(\sqrt{s^{n2} + 1} - s^n)}{h^2 s^n} \right], \quad (2.28)$$

$$c_i^n = \left[\frac{2k(\sqrt{s^{n2} + 1} - s^n)}{h^2 s^n} - \frac{Pe}{2hs^n} \sqrt{\frac{k}{n}} - \frac{k\zeta_i Ste(\sqrt{s^{n2} + 1} - s^n)}{s^n} \frac{(U_{P-2}^n - 4U_{P-1}^n)}{2h^2} \right], \quad (2.29)$$

$$n \geq 0, \quad 1 \leq i \leq P - 1.$$

2.4 Consistency

Since a numerical scheme is problem dependent [118], therefore, the consistency of the numerical scheme for our problem is discussed. A numerical scheme is said to be consistent with a partial differential equation if the local truncation error becomes zero when the step-size of space and time reduce to zero.

Let us denote the Eqs.(2.14)-(2.18) in vector form as

$$\mathcal{X}(\mathcal{Y}(\zeta, t), \mathcal{S}(t)) = (\mathcal{X}_1(\mathcal{Y}(\zeta, t), \mathcal{S}(t)), \mathcal{X}_2(\mathcal{Y}(\zeta, t), \mathcal{S}(t))), \quad (2.30)$$

where

$$\mathcal{X}_1(\mathcal{Y}, \mathcal{S}) = \frac{\partial \mathcal{Y}}{\partial t} - \frac{\zeta}{\mathcal{S}(t)} \frac{d\mathcal{S}}{dt} \frac{\partial \mathcal{Y}}{\partial \zeta} + \frac{Pe}{\mathcal{S}(t)\sqrt{t}} \frac{\partial \mathcal{Y}}{\partial \zeta} - \frac{2(\sqrt{\mathcal{S}^2 + 1} - \mathcal{S})}{\mathcal{S}} \frac{\partial^2 \mathcal{Y}}{\partial \zeta^2}, \quad t > 0, \quad 0 < \zeta < 1 \quad (2.31)$$

$$\mathcal{X}_2(\mathcal{Y}, \mathcal{S}) = \frac{1}{Ste} \frac{d\mathcal{S}}{dt} + 2(\sqrt{\mathcal{S}^2 + 1} - \mathcal{S}) \frac{\partial \mathcal{Y}(1, t)}{\partial \zeta}, \quad t > 0. \quad (2.32)$$

Let us write the vector form of the difference scheme mentioned in the Eqs. (2.22) and (2.25),

$$X(U, s) = (X_1(U, s), X_2(U, s)), \quad (2.33)$$

where X_1 & X_2 are defined at mesh point (ζ_i, t^n) as:

$$X_1(U_i^n, s^n) = \frac{U_i^{n+1} - U_i^n}{k} - \frac{\zeta_i}{s^n} \left(\frac{s^{n+1} - s^n}{k} \right) \left(\frac{U_{i+1}^n - U_{i-1}^n}{2h} \right) + \frac{Pe}{s^n \sqrt{nk}} \left(\frac{U_{i+1}^n - U_{i-1}^n}{2h} \right) - \frac{2s^n(\sqrt{s^{n2} + 1} - s^n)}{s^n} \frac{(U_{i+1}^n - 2U_i^n + U_{i-1}^n)}{h^2}, \quad n \geq 0, \quad 1 \leq i \leq P-1, \quad (2.34)$$

$$X_2(U_i^n, s^n) = \frac{s^{n+1} - s^n}{k} + 2Ste(\sqrt{s^{n2} + 1} - s^n) \frac{(U_{P-2}^n - 4U_{P-1}^n + 3U_P^n)}{2h}, \quad n \geq 0, \quad (2.35)$$

According to [118, 125], the difference scheme $X(U, s)$ is consistent with problem $\mathcal{X}(\mathcal{Y}, \mathcal{S})$ when the local truncation error

$$E_i^n(\mathcal{Y}, \mathcal{S}) = (E(1)_i^n, E(2)_i^n), \quad (2.36)$$

$$E(1)_i^n = X_1(\mathcal{Y}_i^n, \mathcal{S}^n) - \mathcal{X}_1(\mathcal{Y}_i^n, \mathcal{Y}^n), \quad (2.37)$$

$$E(2)_i^n = X_2(\mathcal{Y}_i^n, \mathcal{S}^n) - \mathcal{X}_2(\mathcal{Y}_i^n, \mathcal{S}^n), \quad (2.38)$$

goes to 0 as $h \rightarrow 0$ and $k \rightarrow 0$, where $\mathcal{Y}_i^n = \mathcal{Y}(\zeta_i, t^n)$, and $\mathcal{S}^n = \mathcal{S}(t^n)$ are the exact values of the solution of the Eqs.(2.14)-(2.17).

Let us assume that $\mathcal{Y}(\zeta, t)$ is continuously partial differentiable four times with respect to (w.r.t.) ζ and two times w.r.t. t . Moreover, $\mathcal{S}(t)$ is assumed as two times continuously differentiable function w.r.t. t .

By using Taylor's expansion, expanding $X_1(\mathcal{Y}_i^n, \mathcal{S}^n)$ about (ζ_i, t^n) and using it in Eq.(2.37) which produces:

$$\begin{aligned} E(1)_i^n &= T_i^n(1)k - \frac{\zeta_i}{\mathcal{S}^n} \mathcal{S}'(t^n) T_i^n(2)h^2 - \frac{\zeta_i}{\mathcal{S}^n} \frac{\partial \mathcal{Y}}{\partial \zeta}(\zeta_i, t^n)k - \frac{\zeta_i}{\mathcal{S}^n} T_i^n(4)kh^2 \\ &+ \frac{Pe}{\mathcal{S}^n \sqrt{nk}} T_i^n(2)h^2 - \frac{2\mathcal{S}^n(\sqrt{\mathcal{S}^{n2} + 1} - \mathcal{S}^n)}{\mathcal{S}^n} T_i^n(3)h^2, \end{aligned} \quad (2.39)$$

where

$$T_i^n(1) = \frac{1}{2} \frac{\partial^2 \mathcal{Y}}{\partial t^2}(\zeta_i, t^n), \quad (2.40)$$

$$T_i^n(2) = \frac{1}{6} \frac{\partial^3 \mathcal{Y}}{\partial \zeta^3}(\zeta_i, t^n), \quad (2.41)$$

$$T_i^n(3) = \frac{1}{12} \frac{\partial^4 \mathcal{Y}}{\partial \zeta^4}(\zeta_i, t^n), \quad (2.42)$$

$$T_i^n(4) = \frac{1}{2} \frac{d^2 \mathcal{S}}{dt^2}(t^n). \quad (2.43)$$

Clearly, the local truncation error becomes:

$$E(1)_i^n(\mathcal{Y}, \mathcal{S}) = \mathcal{O}(k) + \mathcal{O}(h^2). \quad (2.44)$$

In the similar manner, we have

$$E(2)_i^n(\mathcal{Y}, \mathcal{S}) = \mathcal{O}(k) + \mathcal{O}(h^2) \quad (2.45)$$

by substituting Eqs.(2.32) and (2.35) in the Eq.(2.38).

Clearly, the technique $X(U, s)$ is consistent with the considered problem $\mathcal{X}(\mathcal{Y}, \mathcal{S})$ with the local truncation error $\mathcal{O}(k) + \mathcal{O}(h^2)$.

2.5 Stability

In this section, the stability of our solution of the problem is discussed. From the Eq.(2.26), the matrix form of the explicit scheme is

$$\mathbf{U}^{n+1} = \mathbf{A}\mathbf{U}^n, \quad n \geq 0, \quad (2.46)$$

where

$$\mathbf{A} = \begin{bmatrix} b_1^n & c_1^n & 0 & 0 & \dots & 0 & 0 \\ a_2^n & b_2^n & c_2^n & 0 & \dots & 0 & 0 \\ 0 & a_3^n & b_3^n & c_3^n & \dots & 0 & 0 \\ \vdots & \vdots & \vdots & \vdots & \ddots & \vdots & \vdots \\ 0 & 0 & 0 & 0 & \dots & a_{P-1}^n & b_{P-1}^n \end{bmatrix},$$

$$\mathbf{U}^n = \begin{bmatrix} U_1^n \\ U_2^n \\ U_3^n \\ \vdots \\ U_{P-1}^n \end{bmatrix} \quad \& \quad \mathbf{U}^{n+1} = \begin{bmatrix} U_1^{n+1} - a_1^n U_0^n \\ U_2^{n+1} \\ U_3^{n+1} \\ \vdots \\ U_{P-1}^{n+1} \end{bmatrix}.$$

The explicit scheme given in Eq.(2.46) is stable if $\|\mathbf{A}\|_\infty \leq 1$. To show this, first, it is needed to show that all the coefficients of Eq. (2.26) are positive under some conditions. By using the Taylor's expansion about $\zeta_P = 1$ as given in [118, 125], we get

$$U_{P-2}^n = 2U_{P-1}^n + \mathcal{O}(h^2), \quad n \geq 0. \quad (2.47)$$

From Eqs.(2.27), (2.47) and by taking into account that $0 \leq \zeta_i < 1$, we have

$$\begin{aligned} \frac{2(\sqrt{s^{n^2} + 1} - s^n)k}{h^2 s^n} - \frac{k Ste(\sqrt{s^{n^2} + 1} - s^n)}{h^2 s^n} U_{P-1}^n &< \frac{2(\sqrt{s^{n^2} + 1} - s^n)k}{h^2 s^{n^2}} \\ &- \frac{k Ste \zeta_i (\sqrt{s^{n^2} + 1} - s^n)}{h^2 s^n} U_{P-1}^n < \frac{2(\sqrt{s^{n^2} + 1} - s^n)k}{h^2 s^{n^2}} \\ &+ \frac{Pe}{2hs^n} \sqrt{\frac{k}{n}} - \frac{k \zeta_i Ste(\sqrt{s^{n^2} + 1} - s^n)}{h^2 s^n} U_{P-1}^n \leq a_i^n. \end{aligned}$$

The coefficient $a_i^n > 0$ if

$$U_{P-1}^n < \frac{2}{Ste}. \quad (2.48)$$

Now, assuming that $s^0 \neq 0$ and taking $s^0 < s^n$, $n \geq 1$, in Eq.(2.28), we get $b_i^n > 0$ if

$$k < \frac{h^2 s^0 (\sqrt{s^{0^2} + 1} + s^0)}{4}. \quad (2.49)$$

From Eqs.(2.29), (2.47) and by considering that $0 \leq \zeta_i < 1$, we have

$$\begin{aligned} \frac{2(\sqrt{s^{n^2} + 1} - s^n)k}{h^2 s^n} - \frac{Pe}{2hs^n} \sqrt{k} &< \frac{2(\sqrt{s^{n^2} + 1} - s^n)k}{h^2 s^n} - \frac{Pe}{2hs^n} \sqrt{\frac{k}{n}} \\ &< \frac{2(\sqrt{s^{n^2} + 1} - s^n)k}{h^2 s^n} - \frac{Pe}{2hs^n} \sqrt{\frac{k}{n}} + \frac{k \zeta_i Ste(\sqrt{s^{n^2} + 1} - s^n)}{h^2 s^n} U_{P-1}^n \leq c_i^n, \quad n \geq 1, \end{aligned}$$

Now, the coefficient $c_i^n > 0$ if

$$Pe < \frac{2\sqrt{k}}{hs^0}, \quad (2.50)$$

where s^0 is a non-zero positive real number and $s^0 < s^n$, $n \geq 1$.

Under the conditions (2.48)-(2.50), all the entries of matrix \mathbf{A} are positive and the

norm infinity of matrix \mathbf{A} is equal to 1. Therefore, the proposed numerical solution is conditionally stable.

2.6 Convergence

In this section, the convergence of the numerical scheme is discussed.

Theorem 2.1. *The finite difference scheme (2.21) for the problem (2.14)-(2.18) is convergent if $\|A\|_\infty \leq 1$.*

Proof Let $U_i^n = \mathcal{Y}_i^n - e_i^n$

where U_i^n is the approximate solution, $\mathcal{Y}_i^n = \mathcal{Y}(\zeta_i, t^n)$, $\mathcal{S}^n = \mathcal{S}(t^n)$ and e_i^n is the error.

From (2.21), we have

$$\begin{aligned} & \frac{(\mathcal{Y}_i^{n+1} - \mathcal{Y}_i^n) - (e_i^{n+1} - e_i^n)}{k} - \frac{\zeta_i}{\mathcal{S}^n} \left(\frac{\mathcal{S}^{n+1} - \mathcal{S}^n}{k} \right) \left(\frac{(\mathcal{Y}_{i+1}^n - \mathcal{Y}_{i-1}^n) - (e_{i+1}^n - e_{i-1}^n)}{2h} \right) \\ & + \frac{Pe}{\mathcal{S}^n \sqrt{nk}} \left(\frac{(\mathcal{Y}_{i+1}^n - \mathcal{Y}_{i-1}^n) - (e_{i+1}^n - e_{i-1}^n)}{2h} \right) = \frac{2(\sqrt{\mathcal{S}^{n2} + 1} - \mathcal{S}^n)}{\mathcal{S}^n} \\ & \frac{(\mathcal{Y}_{i+1}^n - 2\mathcal{Y}_i^n + \mathcal{Y}_{i-1}^n) - (e_{i+1}^n - 2e_i^n + e_{i-1}^n)}{h^2}, \quad n \geq 0, \quad 1 \leq i \leq P-1, \end{aligned} \quad (2.51)$$

According to the Taylor's series expansion, the Eq. (2.51) gives

$$\begin{aligned} & \left(\frac{\partial \mathcal{Y}(\zeta_i, t^n)}{\partial t} + \mathcal{O}(k) - \frac{(e_i^{n+1} - e_i^n)}{k} \right) - \frac{\zeta_i}{\mathcal{S}^n} \left(\frac{d\mathcal{S}(t^n)}{dt} + \mathcal{O}(k) \right) \left(\frac{\partial \mathcal{Y}(\zeta_i, t^n)}{\partial \zeta} + \mathcal{O}(h^2) \right) \\ & - \frac{(e_{i+1}^n - e_{i-1}^n)}{2h} \left) + \frac{Pe}{\mathcal{S}^n \sqrt{nk}} \left(\frac{\partial \mathcal{Y}(\zeta_i, t^n)}{\partial \zeta} + \mathcal{O}(h^2) - \frac{(e_{i+1}^n - e_{i-1}^n)}{2h} \right) = \frac{2(\sqrt{\mathcal{S}^{n2} + 1} - \mathcal{S}^n)}{\mathcal{S}^n} \\ & \left(\frac{\partial^2 \mathcal{Y}(\zeta_i, t^n)}{\partial \zeta^2} + \mathcal{O}(h^2) - \frac{(e_{i+1}^n - 2e_i^n + e_{i-1}^n)}{h^2} \right), \quad n \geq 0, \quad 1 \leq i \leq P-1, \end{aligned} \quad (2.52)$$

Thus, we have

$$\begin{aligned} & \frac{(e_i^{n+1} - e_i^n)}{k} - \frac{\zeta_i}{\mathcal{S}^n} \frac{d\mathcal{S}(t^n)}{dt} \frac{(e_{i+1}^n - e_{i-1}^n)}{2h} + \frac{Pe}{\mathcal{S}^n \sqrt{nk}} \frac{(e_{i+1}^n - e_{i-1}^n)}{2h} = \frac{2(\sqrt{\mathcal{S}^{n^2} + 1} - \mathcal{S}^n)}{\mathcal{S}^n} \\ & \frac{(e_{i+1}^n - 2e_i^n + e_{i-1}^n)}{h^2} + \mathcal{O}(k + h^2), \quad n \geq 0, \quad 1 \leq i \leq P-1, \end{aligned} \quad (2.53)$$

With the help of boundary condition (2.23), the matrix form of Eq. (2.53) can be written as

$$\mathbf{E}^{n+1} = \mathbf{A}\mathbf{E}^n + \mathbf{B}, \quad n \geq 0, \quad (2.54)$$

where

$$\mathbf{E}^{n+1} = \begin{bmatrix} e_1^{n+1} \\ e_2^{n+1} \\ e_3^{n+1} \\ \vdots \\ e_{P-1}^{n+1} \end{bmatrix}, \quad \mathbf{E}^n = \begin{bmatrix} e_1^n \\ e_2^n \\ e_3^n \\ \vdots \\ e_{P-1}^n \end{bmatrix}, \quad \mathbf{B} = k\mathcal{O}(k + h^2) \begin{bmatrix} 1 \\ 1 \\ 1 \\ \vdots \\ 1 \end{bmatrix},$$

and \mathbf{A} is the square matrix given in Eq. (2.46).

$$\|\mathbf{E}^{n+1}\|_\infty \leq \|\mathbf{A}^{n+1}\|_\infty \|\mathbf{E}^0\|_\infty + (\|\mathbf{A}^n\|_\infty + \|\mathbf{A}^{n-1}\|_\infty + \dots + \|I\|_\infty) \|\mathbf{B}\|_\infty, \quad n \geq 0, \quad (2.55)$$

As $\mathbf{E}^0 = 0$ and $\|\mathbf{A}\|_\infty \leq 1$, hence, Eq. (2.55) becomes

$$\|\mathbf{E}^{n+1}\|_\infty \leq (n+1)k|\mathcal{O}(k + h^2)|.$$

Consequently, $|e_i^{n+1}| \rightarrow 0$ as $h \rightarrow 0$ and $k \rightarrow 0$ which proves that U converges to \mathcal{Y} when $\|\mathbf{A}\|_\infty \leq 1$.

2.7 Results and Discussions

As per our knowledge, the exact solution of the problem (2.8)-(2.12) is not available in the literature for the non-zero ϵ . Since, $2s(\sqrt{s^2 + 1} - s)$ converges to 1 when s is sufficiently large ($s \geq 2$). Therefore, approximating $2s(\sqrt{s^2 + 1} - s) \approx 1$ and taking $\epsilon = 0$ in the Eqs. (2.8)-(2.12), the exact solution of this particular case [110] of the problem (2.8)-(2.12) becomes

$$T(x, t) = \frac{e^{(Pe-\lambda)^2} \sqrt{\pi} \lambda (erf(Pe - \frac{x}{2\sqrt{t}}) - erf(Pe - \lambda))}{Ste}, \quad (2.56)$$

$$s(t) = 2\lambda\sqrt{t}, \quad (2.57)$$

where $erf(\cdot)$ denotes the error function and the value of the constant λ can be found by the following transcendental equation:

$$\frac{e^{(Pe-\lambda)^2} \sqrt{\pi} \lambda (erf(Pe - \frac{x}{2\sqrt{t}}) - erf(Pe - \lambda))}{Ste} = 1. \quad (2.58)$$

To show the existence of the solution of the problem (2.8)-(2.12), let us define a function

$$g(\lambda) = \frac{e^{(Pe-\lambda)^2} \sqrt{\pi} \lambda (erf(Pe - \frac{x}{2\sqrt{t}}) - erf(Pe - \lambda))}{Ste} - 1 \quad (2.59)$$

Clearly, the function $g(\lambda)$ is continuous and differentiable in the interval $(0, \infty)$. Also, $\lim_{\lambda \rightarrow 0^+} g(\lambda)$ is a negative real number and $\lim_{\lambda \rightarrow \infty} g(\lambda)$ is positive real number which shows that there exists atleast one root of $g(\lambda)$ in the interval $(0, \infty)$. Besides this, the derivative of the function $g(\lambda)$ is always positive in the interval $(0, \infty)$ under the condition $Pe \leq \sqrt{2}$ which shows that the function $g(\lambda)$ has unique root in the interval $(0, \infty)$.

To initiate the numerical procedures and to avoid the singularity at time 0, *i.e.* $s(0) = 0$, the exact solutions of the temperature and moving phase given by Eqs.(2.56)-(2.57) are used for a short time $t = 0.1$. The similar procedure has been already used for initial guess in the numerical solutions of some moving boundary problems([114], [66] and [121]).

In order to achieve the stability of the scheme, all the computations have been made by taking the initial time $t = 0.1$, grid size $h = 0.1$ ($P = 10$ or $\Delta\zeta = \frac{1}{10}$) and the time step $k = 0.0001$.

For a particular case ($2s(\sqrt{s^2 + 1} - s) = 1$ and $\epsilon = 0$), the validation of the accuracy of the solution is shown through Tables 2.1-2.2. In Table 2.1, the relative error between exact and obtain numerical solution of the temperature profile at time $t = 10$ are presented for three different cases, *i.e.* ($Pe = 0.5, Ste = 0.1$), ($Pe = 0.25, Ste = 0.25$) and ($Pe = 0.1, Ste = 0.5$). Table 2.2 depicts the comparison of the exact and numerical solutions of the position of the moving interface at different times for the same earlier three cases. From Tables 2.1-2.2, it is seen that the solution obtained by numerical scheme is nearly equal to the exact.

The dependence of temperature profile and tracking of moving boundary on various parameters are shown in Figs. 2.1 - 2.8. Figs. 2.1 and 2.2 represent the tracking of melting phase front for three different Stefan numbers ($Ste = 0.2, 0.5, 0.8$) with the fixed Peclet number ($Pe = 0.5$) and frequency ($\omega = \pi/2$) for amplitudes 0.5 and 0.75, respectively. From these two figures, it is obtained that the evolution of the moving interface increases rapidly with the increment of the Stefan number which is similar to the result of Savovic and Caldwell [66]. The effects of Peclet numbers on tracking of the moving melting front are shown in Figs. 2.3 and 2.4 at the fixed value of $Ste = 0.5, \omega = \pi/2$ for two oscillating amplitudes $\epsilon = 0.5$ and $\epsilon = 0.75$, respectively. Figs. 2.3-2.4 depict that the movement of the moving interface becomes faster with

the increment of Peclet number. Hence, the melting process becomes fast when we increase either Stefan number or Peclet number or both. However, the effect of the Peclet number on the movement of moving melting front is lesser than the Stefan number. From Figs. 2.1 - 2.4, it is also seen that the moving boundary periodically moves with larger oscillating amplitudes for larger value of ϵ .

Figs. 2.5 and 2.6 represent the temperature distribution for different times ($t = 20$, $t = 21$, $t = 22$, $t = 23$) at the fixed parameters $Ste = 0.2$, $Pe = 0.5$, $\omega = \pi/2$ for two different oscillation amplitudes $\epsilon = 0.5$ and $\epsilon = 0.75$, respectively. From the Figs. 2.5 and 2.6, the effect of the oscillating amplitude on temperature profile at the first boundary, *i.e.* $\zeta = 0$ can be clearly observed and it is seen that the change of temperature profile in the whole domain is more effective for larger oscillating amplitude. In Figs. 2.7 and 2.8, the trajectory of moving melting front and temperature profile are shown for the Stefan problem with periodic boundary condition for three different cases, *i.e.*, Stefan problem with constant thermal conductivity (Standard problem), Stefan problem with moving phase change material and constant thermal conductivity ($\kappa = 1$), and Stefan problem with moving phase change material and size dependent thermal conductivity ($\kappa(s(t))$). From Fig. 2.7, it is observed that the speed of moving melting front becomes faster in case of Stefan problem with moving PCM than the standard problem. For the Stefan problem with moving PCM, it is also seen that the moving melting front becomes slower in the case of size dependent thermal conductivity than the constant thermal conductivity. In Fig. 2.8, the deviation of temperature profile is observed if we compare the problem with moving PCM and standard problem (problem without moving PCM). For the Stefan problem with moving PCM, it is also observed from the Fig. 2.8 that the variable thermal conductivity $\kappa(s(t))$ does not produce much effect on temperature profile of the problem in comparison to the problem with constant thermal conductivity

($\kappa = 1$).

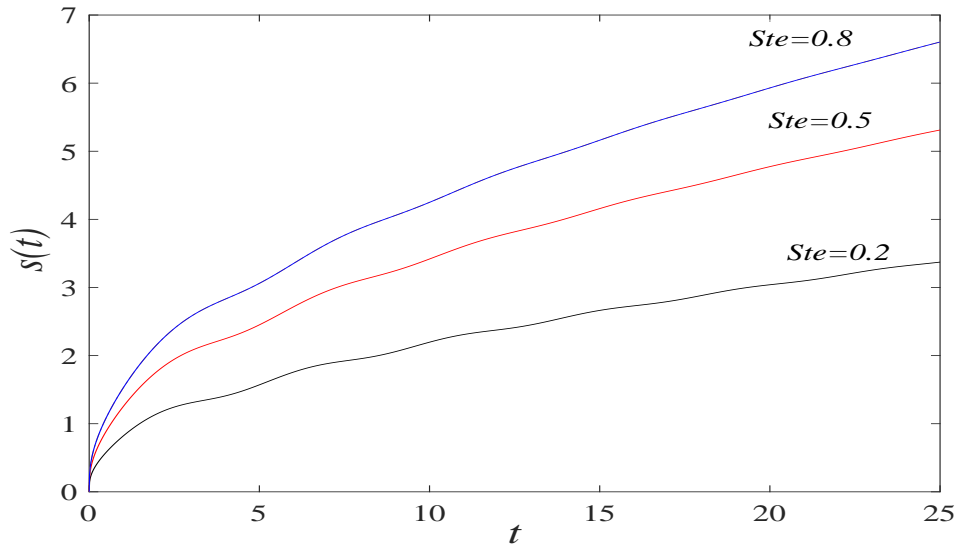


FIGURE 2.1: Dependence of moving melting front on Stefan number at $\epsilon = 0.5$.

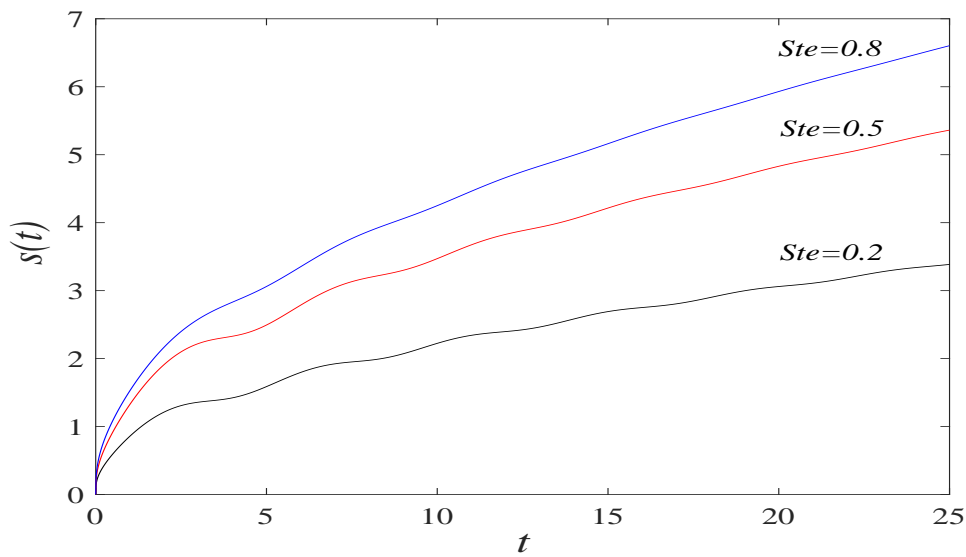


FIGURE 2.2: Dependence of moving melting front on Stefan number at $\epsilon = 0.75$.

TABLE 2.1: Temperature distribution at $t = 10$ for different parameters.

<i>S.No.</i>	<i>Parameters</i>	ζ	U_{exact}	$U_{numerical}$	<i>Relative Error</i>
1	$Pe = 0.5$ $Ste = 0.1$	0.0	1.000000	1.000000	0.000000
		0.1	0.908439	0.90851	7.83×10^{-5}
		0.2	0.81482	0.814952	1.62×10^{-4}
		0.3	0.719207	0.719383	2.44×10^{-4}
		0.4	0.62166	0.621864	3.28×10^{-4}
		0.5	0.522249	0.522464	4.12×10^{-4}
		0.6	0.421048	0.421257	5.07×10^{-4}
		0.7	0.318136	0.31832	5.78×10^{-4}
		0.8	0.213597	0.213739	6.62×10^{-4}
		0.9	0.107521	0.107601	7.4×10^{-4}
		1.0	0.000000	0.000000	0.000000
2	$Pe = 0.25$ $Ste = 0.25$	0.0	1.000000	1.000000	0.000000
		0.1	0.90377	0.903823	5.85×10^{-5}
		0.2	0.806067	0.80616	1.15×10^{-4}
		0.3	0.707115	0.707237	1.72×10^{-4}
		0.4	0.60715	0.607289	2.29×10^{-4}
		0.5	0.506416	0.50656	2.83×10^{-4}
		0.6	0.405161	0.405297	3.37×10^{-4}
		0.7	0.303637	0.303755	3.89×10^{-4}
		0.8	0.2021	0.202188	4.37×10^{-4}
		0.9	0.100803	0.100852	4.87×10^{-4}
		1.0	0.000000	0.000000	0.000000
3	$Pe = 0.1$ $Ste = 0.5$	0.0	1.000000	1.000000	0.000000
		0.1	0.896872	0.896889	1.9×10^{-6}
		0.2	0.793227	0.793255	3.75×10^{-5}
		0.3	0.689532	0.689569	5.41×10^{-5}
		0.4	0.586254	0.586294	6.78×10^{-5}
		0.5	0.483854	0.483892	7.78×10^{-5}
		0.6	0.38278	0.382813	8.59×10^{-5}
		0.7	0.283464	0.28349	9.07×10^{-5}
		0.8	0.186314	0.186331	9.27×10^{-5}
		0.9	0.0917102	0.0917185	9.10×10^{-5}
		1.0	0.000000	0.000000	0.000000

TABLE 2.2: Positions of the moving boundary for different time with different parameters.

<i>Sr.No.</i>	<i>Parameters</i>	<i>t</i>	<i>s_{exact}</i>	<i>s_{numerical}</i>	<i>Relative Error</i>
1	<i>Ste</i> = 0.1 <i>Pe</i> = 0.5	1	0.46521	0.494588	6.31×10^{-2}
		2	0.65791	0.679843	3.33×10^{-2}
		3	0.80577	0.824251	2.29×10^{-2}
		4	0.93042	0.946729	1.75×10^{-2}
		5	1.04024	1.05506	1.42×10^{-2}
		6	1.13953	1.15324	1.20×10^{-2}
		7	1.23083	1.24367	1.04×10^{-2}
		8	1.31581	1.32794	9.21×10^{-3}
		9	1.39563	1.40717	8.26×10^{-3}
		10	1.47112	1.48216	7.5×10^{-3}
2	<i>Ste</i> = 0.25 <i>Pe</i> = 0.25	1	0.70878	0.75095	5.95×10^{-2}
		2	1.00236	1.03365	3.12×10^{-2}
		3	1.22764	1.25393	2.14×10^{-2}
		4	1.41755	1.44079	1.64×10^{-2}
		5	1.58487	1.60599	1.33×10^{-2}
		6	1.73614	1.75571	1.12×10^{-2}
		7	1.87525	1.89360	9.78×10^{-3}
		8	2.00472	2.02210	8.67×10^{-3}
		9	2.12633	2.14289	7.79×10^{-3}
		10	2.24135	2.25721	7.07×10^{-3}
3	<i>Ste</i> = 0.5 <i>Pe</i> = 0.1	1	0.949508	1.0013	5.54×10^{-2}
		2	1.34281	1.38082	2.41×10^{-2}
		3	1.6446	1.67631	1.92×10^{-2}
		4	1.89902	1.92695	1.47×10^{-2}
		5	2.12316	2.14854	1.19×10^{-2}
		6	2.32581	2.34927	1.01×10^{-2}
		7	2.51216	2.53415	8.75×10^{-3}
		8	2.68561	2.70642	7.75×10^{-3}
		9	2.84852	2.86835	6.96×10^{-3}
		10	3.00261	3.02163	6.33×10^{-3}

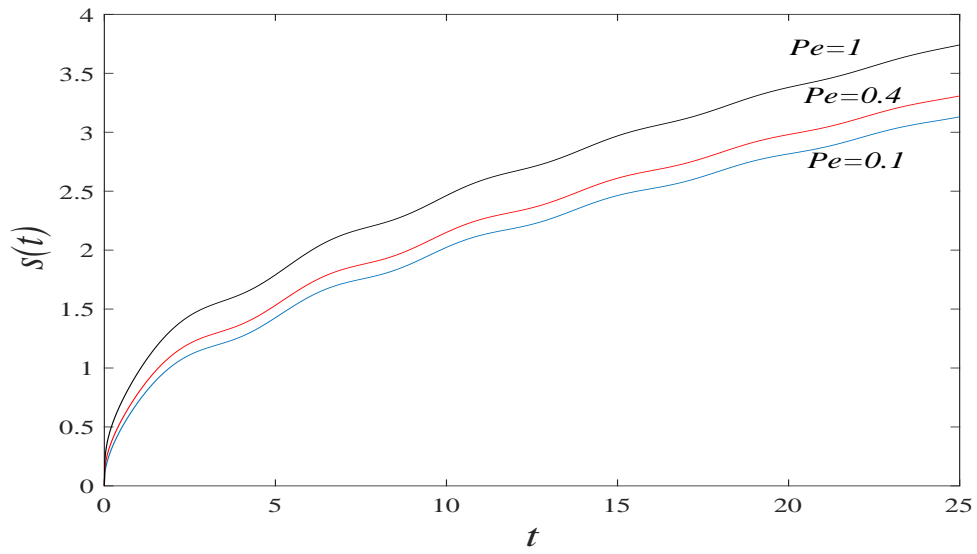


FIGURE 2.3: Evolution of moving melting front for different Peclet number at $\epsilon = 0.5$.

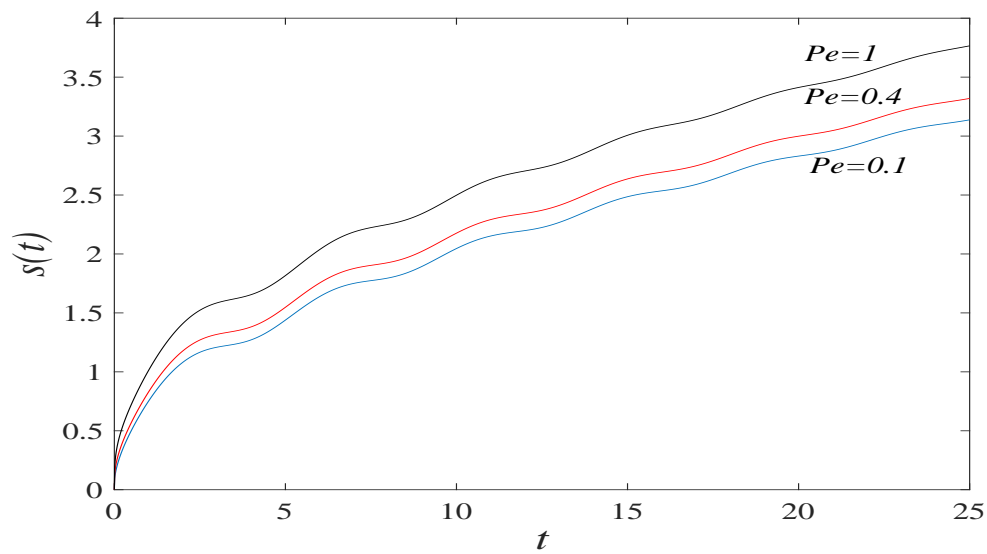


FIGURE 2.4: Evolution of moving melting front for different Peclet number at $\epsilon = 0.75$.

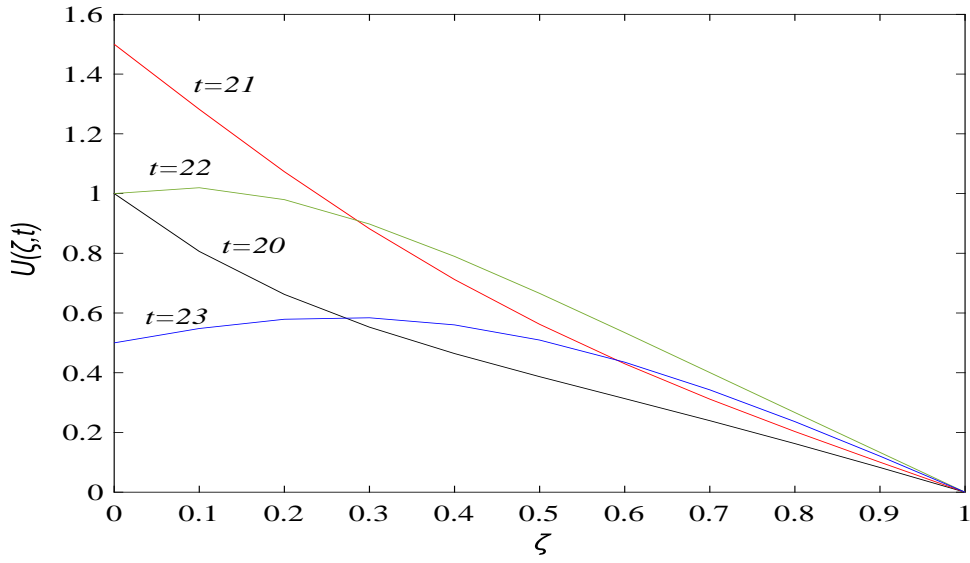


FIGURE 2.5: Temperature profile for different times at $\epsilon = 0.5$.

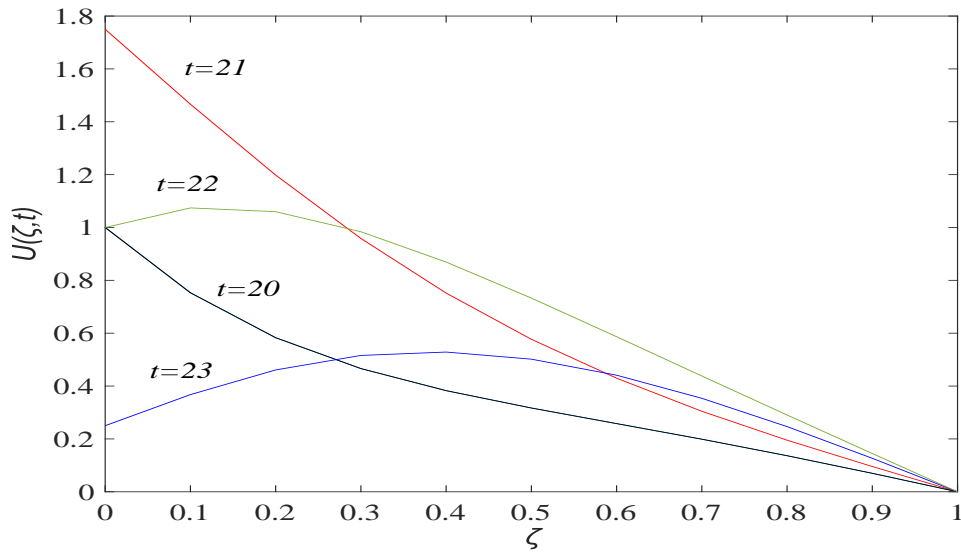


FIGURE 2.6: Temperature profile for different times at $\epsilon = 0.75$.

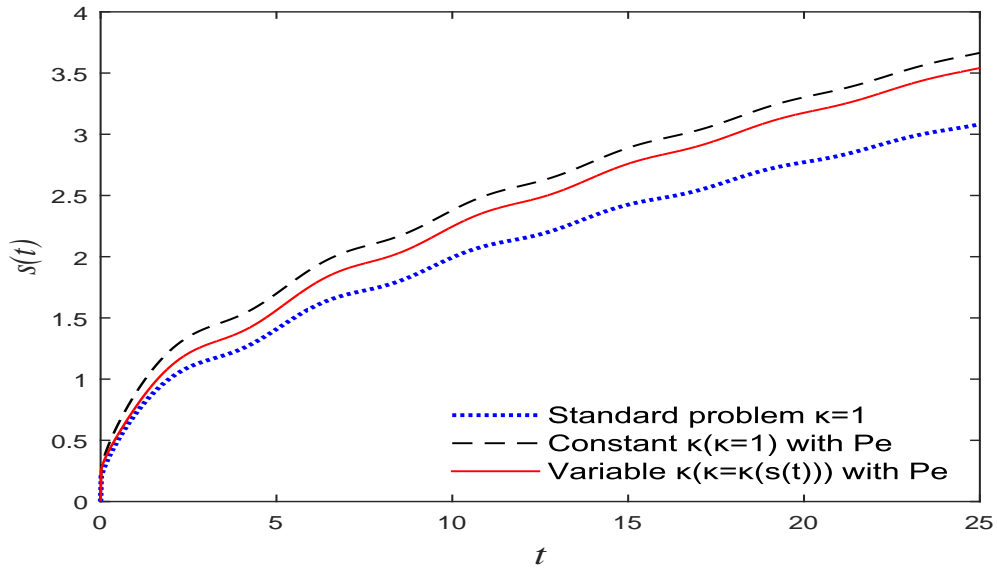


FIGURE 2.7: Comparison of moving melting front at $Pe = 1$, $Ste = 0.2$, $\epsilon = 0.5$ and $\omega = \pi/2$.

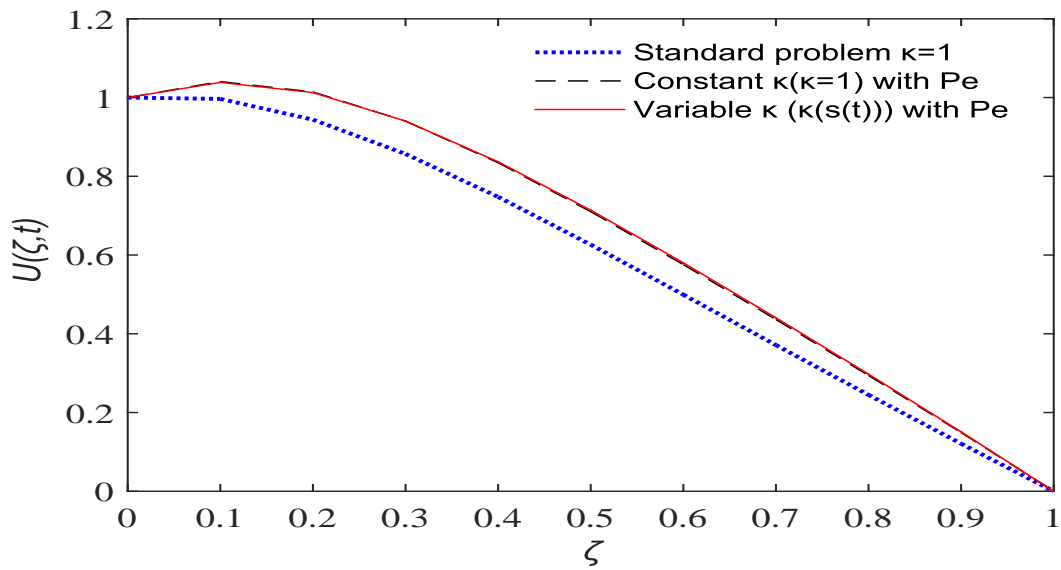


FIGURE 2.8: Comparison of temperature profile at $Pe = 1$, $Ste = 0.2$, $\epsilon = 0.5$, $\omega = \pi/2$ and $t = 22$.

2.8 Conclusion

In this chapter, a finite difference scheme is successfully applied to present a numerical solution of a melting problem with moving phase change material and size-dependent thermal conductivity. From this study, it is observed that the numerical approach is simple and sufficiently accurate for the solution of wide class of the Stefan problems. It is found that the moving melting front and temperature profile are affected by the Stefan number (Ste), Peclet number (Pe) and size-dependent thermal conductivity ($\kappa(s(t))$). But, the effect of Stefan number is more pronounced than the Peclet number and size-dependent thermal conductivity. For a Stefan problem with moving PCM, it is seen that the melting process becomes slower in the case of size-dependent thermal conductivity than that of constant thermal conductivity. However, the melting process becomes fast for large values of Peclet numbers or/and Stefan number. It is also observed that the presence of moving PCM increases the melting process or the movement of melting interface. For $2s(\sqrt{s^2 + 1} - s) \approx 1$ and $\epsilon = 0$, the problem reduces to a special case of [111] and the solution of the moving melting front becomes proportional to \sqrt{t} which is similar to classical Stefan problem [100].
